COBEM 2023 27TH INTERNATIONAL CONGRESS OF MECHANICAL ENGINEERING

ABCM Brazilian Society of Mechanical Sciences and Engineering
27th ABCM International Congress of Mechanical Engineering
December 04-08, 2023, Florianópolis-SC, Brazil

COB-2023-2177
EXPERIMENTAL STUDY OF BOUNDARY LAYER TRANSITION INFLUENCED BY A BUMP

Lenz Lopez Lazaro
Victor Barcelos Victorino
USP, EESC, SAA
lenzjll@usp.br, barcelos.victorino@usp.br

Felipe Oliveira Aguirre
felipe.aguirre@usp.br

Marcello Augusto Faraco de Medeiros
marcello@sc.usp.br

Abstract. *Real aircraft often exhibit surface irregularities, such as bumps, which can lead to a decrease in performance due to the anticipated transition of the boundary layer. Thus, this paper presents an experimental investigation of the effects of a two-dimensional bump on boundary layer transition dominated by Tollmien-Schlichting (T-S) waves. The objective of this research is to understand the influence of a 2D bump on the dynamics of T-S growth and the transition from laminar to turbulent flow. The experiments were carried out at the Low Acoustic Noise and Turbulence (LANT) wind tunnel from the School of Engineering of São Carlos, University of São Paulo. Hot-wire anemometry was employed to measure mean and fluctuation velocity. Concerning the detection of the transition location, a Preston tube was applied. The experimental rig consists of an aluminum flat plate with a chord of 2.32 m featuring a bump in x=0.6 m with adjustable height, with a maximum stroke of 20 mm. The results of this study are expected to provide insights into the effects of surface irregularities on aircraft performance and could lead to improved design strategies for future aircraft.*

Keywords: *Boundary Layer Transition, Tollmien-Schlichting (T-S) waves, bump*

1. INTRODUCTION

The effects caused by imperfections on the surface of aircraft have been studied for many years. The behavior of the transition from laminar to turbulent flow is strongly influenced by various surface irregularities, such as steps, cavities, and protrusions, which are commonly encountered in practice. These imperfections are analyzed using different approaches in various areas of aeronautics. This includes cases where these surface imperfections on an aircraft lead to an increased amplification of Tollmien-Schlichting TS waves, anticipating the transition to turbulence and consequently causing a drastic increase in the drag coefficient. Furthermore, there are transition phenomena that deviate from the growth of TS waves and are thus referred to as bypass transition, as cited by (Morkovin, 1985). Furthermore, Morkovin expresses, as well as (Reshotko, 2001), that by pass transition is inherently nonlinear.

The motivation behind this work is the reduction of the drag coefficient in aircraft, which will bring significant benefits to the aerospace industry. For example, a substantial reduction in fuel consumption can be achieved in commercial aircraft, leading to lower costs associated with fuel consumption. Additionally, the aircraft's payload can be dramatically increased, resulting in improved performance and increased flight range. According to (Reneaux, 2004), approximately 22% of airline costs are attributed to fuel consumption. Important estimates provided by (Schneider, 2001) quantify that a hypothetical 1% reduction in the total aerodynamic drag of a large commercial aircraft operating over long distances would result in savings of $400,000$ liters of fuel and a reduction of $5,000$ kg of harmful emissions per year.

Regarding boundary layer instability and transition, (Tollmien, 1928) and (Schlichting, 1933) worked on the development of Linear Stability Theory, which is based on the viscous instability of the laminar boundary layer of Blasius profile for small-amplitude disturbances. From this perspective, (Schubauer and Skramstad, 1947) were the first to experimentally demonstrate transition dominated by the growth of Tollmien-Schlichting TS waves. Their experiment confirmed the existence of TS waves, their connection to transition, and the quantitative description of their behavior by the Tollmien and Schlichting theory. Regarding transition prediction, (van Ingen, 1956) and (Smith and Gamberony, 1956) correlated experimental results with linear stability theory. As a result, they developed the e^N method, capable of predicting transition when the integral growth of T-S waves reaches a factor of $N = 9$.

On the other hand, the initial experimental studies of the effects of surface roughness have been addressed by (Tani *et al.*, 1940), (Stuper, 1949), and (Dryden, 1949). These experiments demonstrated the influence of the roughness height

on the transition Reynolds number, which is upstream displacement as the roughness height increases. (Klebanoff and Tidstrom, 1972) indicated that these imperfections have a destabilizing effect in the recovery region, i.e., the region of the distorted mean flow immediately downstream of the roughness element. This leads to the transition occurring upstream compared to the case without roughness. Results from (Wang and Gaster, 2005) demonstrate that backward-facing steps are more destabilizing compared to forward-facing steps. The work of (Crouch and Kosorygin, 2020) employed experiments to quantify and model the impact on the integral growth of Tollmien-Schlichting TS waves (factor N) based on step heights (both forward and backward-facing) and rectangular bump. Starting from the relationship developed for steps, the estimation of the variation of factor N with respect to the height of a rectangular bump showed a good fit with the linear superposition of forward and backward facing steps.

The present study aims to experimentally examine the influence of a bump, with variable height, on boundary layer transition. Initially, pressure distribution on the wall were measured for the smooth case (no bump) and also for bumps of different heights in order to located the transition point. In addition, to mapping the T-S wave evolution, velocity fluctuation acquisitions were taken within the boundary layer. Finally, the results were compared with the linear stability theory.

2. EXPERIMENTAL SETUP

The experiments were conducted in the Low Noise and Turbulence Wind Tunnel (LANT) Fig. 1 at EESC-USP. The closed circuit wind tunnel has a test section with transverse dimensions of 1.00 m $\times$ 1.00 m and a length of 3.00 m. In Tab. 1, it can be observed that, for different free-stream flow velocities measured at the empty test section and with the model installed, turbulence intensities vary slightly within a frequency range of 1 to 1024 Hz. Furthermore, several devices can be found within LANT to enhance flow uniformity, reduce turbulence intensity, and background acoustic noise. A detailed overview of the design and performance of the LANT wind tunnel is provided in (Amaral, 2021).

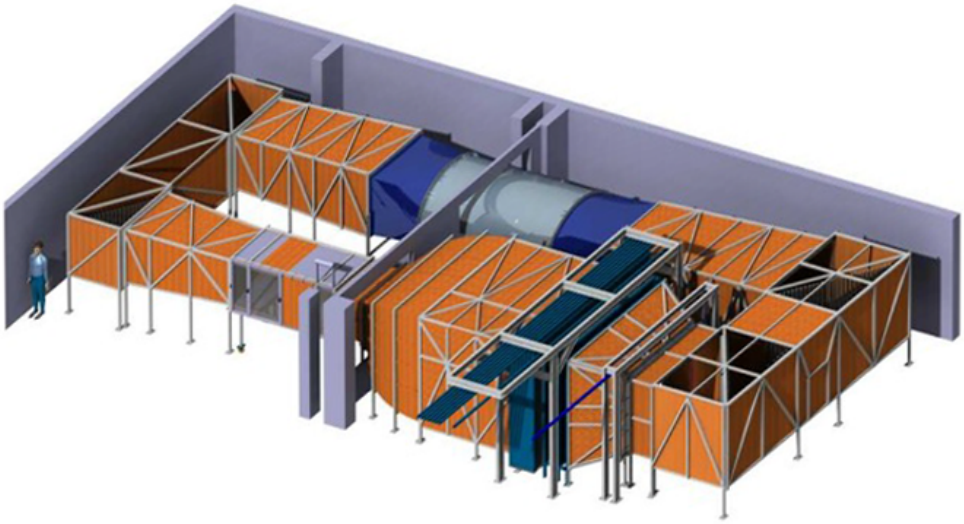

Figure 1. LANT wind tunnel aerodynamic circuit Iso-Metric view.

Table 1. Free-stream turbulence intensity measured in different conditions.

U_∞ **[m/s]**	Tu **%**	**Frequency Range [Hz]**	**Test Section**
10	0,041	1 - 1024	Empty
15	0.040	1 - 1024	Empty
20	0.038	1 - 1024	Empty
27	0.077(0.054)	1 - 1024(4 - 1024)	Installed Model

Inside the test section, a model of a flat plate was installed as indicated in the schematic shown in Fig. 2. The leading edge, item (1) in Fig. 2, is the region of stagnation (high static pressure) due to the deceleration of the incident flow. The dimensions of the flat plate item (2) in Fig. 2 is 2 m in length, 999 mm in wingspan, and 100 mm in thickness, and it is positioned vertically in the test section. The interchangeable protrusion system, item (3) in Fig. 2, coupled to the flat plate to 600 mm from the leading edge, houses the mechanisms needed to alter the geometry. The protrusion measures 30 mm in length and 600 mm in wingspan with a adjustable height of 20 mm that can be moved inwards to create a gap or outwards to create a bump. Finally, two control surfaces attached to the model's trailing edge allow the fine-tuning of the pressure distribution, the flap, and tab, items (4) of Fig. 2.

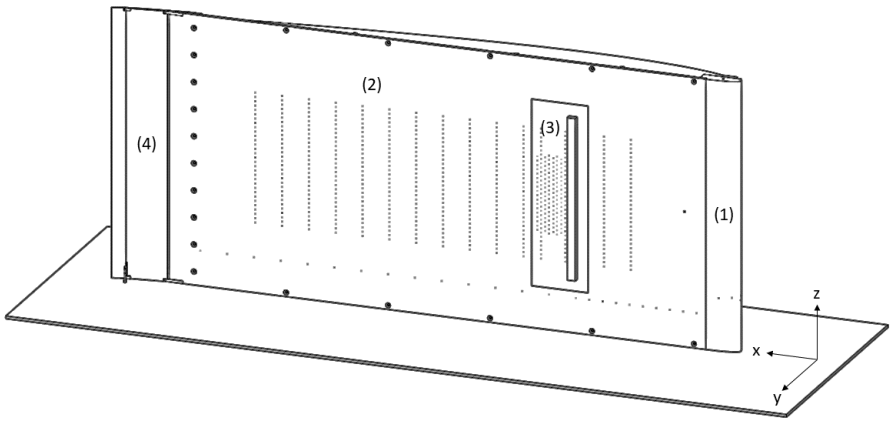

Figure 2. Isometric view of the test model. (1) Leading-edge; (2) Flat plate; (3) Protrusion system; (4) Flap and tab.

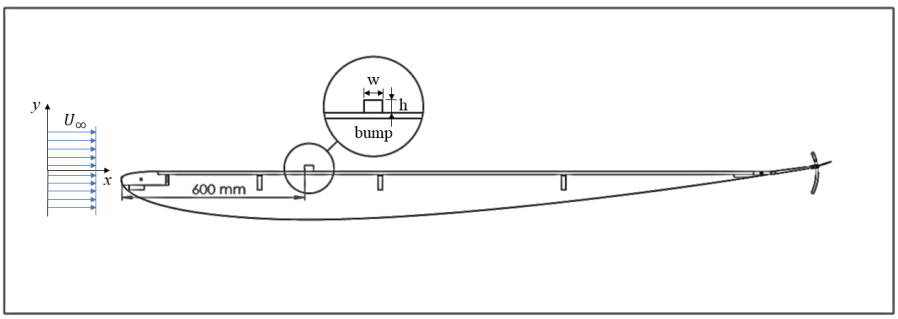

Figure 3. Schematic illustrating of the placement of the bump model and the reference system for the free stream velocity direction.

2.1 Preston tube

To estimate the transition location, a round Preston tube with a diameter of 0.9 mm Fig. 5 was used to measure the total pressure near the plate surface. This measurement is proportional to the skin friction coefficient, allowing the measurement of the increase in friction in the laminar regime up to the transition to turbulence. Therefore, the minimum value within the laminar regime represents the location of the transition. Furthermore, a wing model was designed to cover the rail, specifically adapted to house the Preston tube apparatus. Figure. 4 below, a clear view of the assembly is shown. The needle of the Preston tube was bent towards the flat plate, similar to the HWA probe, and positioned with a slight angle of contact with the flat plate. By using an LVDT (Linear Variable Differential Transformer) distance sensor installed at the tip of the wing, it was possible to maintain a constant angle of the needle across different runs. The wing also covers the pneumatic hoses of both devices. All the wing's holes and indentations were covered with tape to prevent unwanted acoustic resonance or other oscillatory phenomena. The sensitive element consists of a Honeywell TruStability differential pressure sensor, model 004ND, which has a total error range of 4.97 Pa. The sensor is connected to an Arduino board, and the data is read by a MATLAB function.

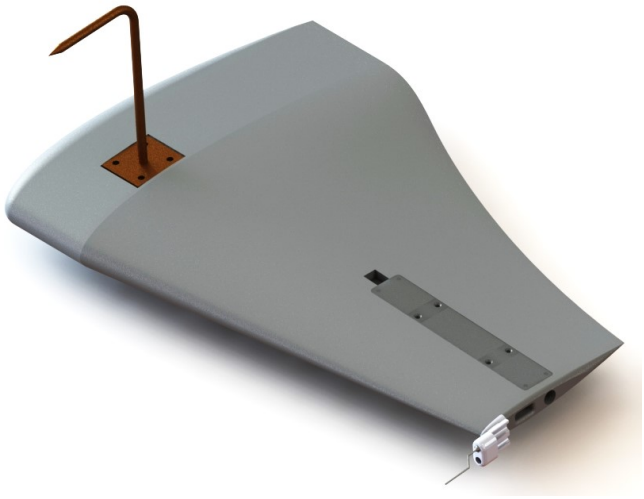

Figure 4. Wing model houses both the Pitot tube(left) and Preston tube(right) probes.

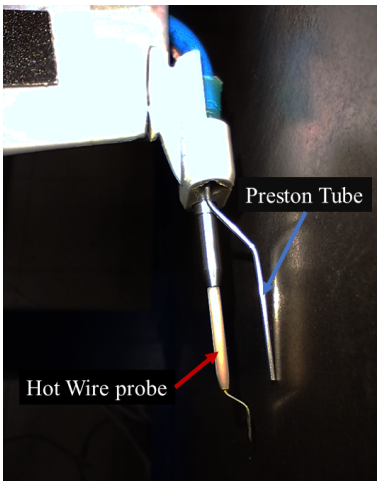

Figure 5. Preston tube probe near the plate surface.

2.2 Hot wire Anemometry

To obtain relevant measurements, such as pressure, temperature, and velocity, a wide range of highly sensitive instruments were used. Hot-Wire Anemometry was the chosen technique for velocity measurements. The anemometer circuit used was the AN-1002 from A.A. Lab System Fig. 6, and the hot wire probe Fig. 7, was the miniature wire boundary layer probe 55P15 from Dantec Dynamics. The voltage signal is derived and sent to two data acquisition modules, one for mean velocity (DC voltage) and the other for fluctuating velocity (AC voltage). The first one is a National Instruments USB-DAQ 6002 with 16-bit resolution and a maximum sampling rate of up to 50 kSamples/s on the analog input channels and 5 kSamples/s on the analog output channels. The second one consists of a set of 7 PXI-4496/98 boards with 24-bit resolution installed in a PXI-1042Q chassis, all from National Instruments. While these boards are used for data acquisition from microphones, one of them is used for recording fluctuating velocity due to its better resolution compared to the USB-DAQ 6002. Signal conditioning and manipulation were performed using MATLAB. The probe's position within the test section was controlled by a three-axis positioning mechanism.

Figure 6. Anemometer circuit AN-1002 from A.A. Lab System.

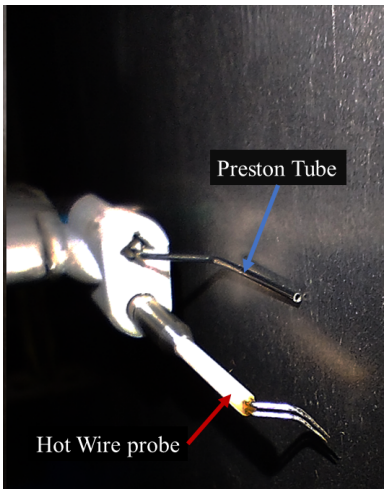

Figure 7. Hot wire probe near the plate surface.

3. RESULTS

To begin, was demonstrate in this experiment that the flat plate follows the Blasius boundary layer profile. For this experiment, an anemometer was used, but before was employed a calibration of the voltage and velocity Fig. 8. The conversion from voltage to velocity was done using King's Law, $E^2 = A + BU^n$, where A, B, and n are constants obtained from the least-squares regression. To map the velocity profile were taken 41 steps along the y-axis of 0.2 mm for different x-stations. The data acquisition time was 8 seconds per step with a sampling rate of 2048 Hz. Then, a graph of η against normalized velocity U/U_∞ was plotted, where $\eta = y\sqrt{U_\infty/\nu x}$. The flow passing through the flat plate behaves in a laminar manner for velocities of 17 m/s, 26 m/s, and 28 m/s for $x = 0.4$ m, $x = 0.6$ m, and $x = 1.0$ m as display Fig. 9 respectively. Let us observe that the experimental results closely match the theoretical curve derived from the Blasius equation solution.

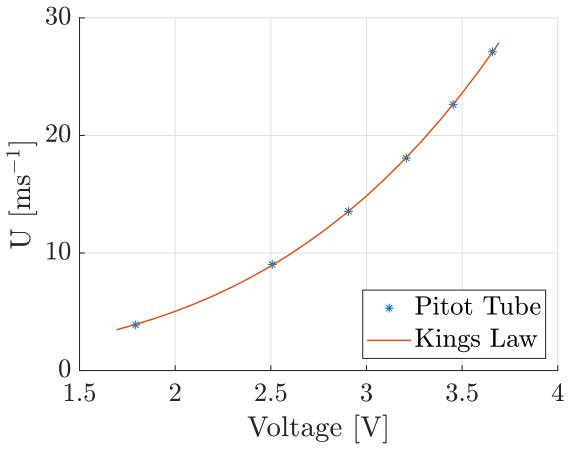

Figure 8. Calibration curve.

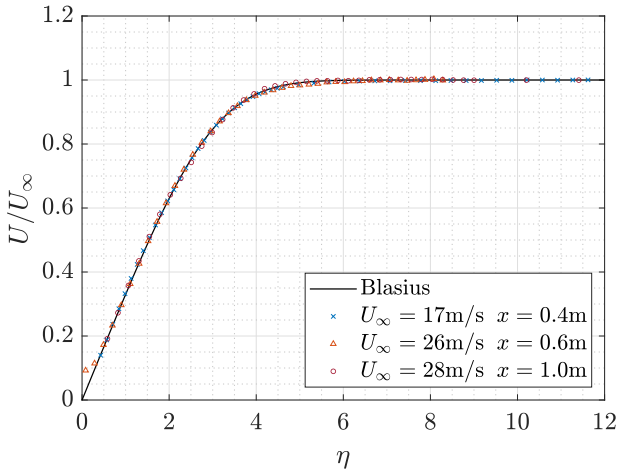

Figure 9. Blasius for several velocities and x-stations.

3.1 The Transition Location

The transition location was determined using a Preston tube technique as described on the previous section, which is moved along the x direction, where the probe is situated on the centerline of the flat plate i.e in the middle of the span (z-axis). The total pressure measured by the instrument is related to the velocity profile near the plate surface. The transition location is determined based on the distribution of the minimum total pressure. An experiment was conducted using a smooth plate as the reference point and a bump of 0.25 mm (see Fig. 10). The free-stream velocity was 27.2 m/s, and the Reynolds number based on the displacement thickness over the smooth plate for $x = 0.6$ m (where the bump begins) was $Re_{\delta^\star} = 1635$. The Preston tube is then placed into contact with the plate wall, starting the drift from the end point defined at $x = 1900$ mm near the trailing edge. Furthermore, the Preston tube is moved towards the bump with a grid of 36 steps up to $x = 640$ mm. For the smooth surface, it can be observe that the natural transition occurred at 1700 m Fig. 7 while for $h = 0.25$ mm the transition location is at $x = 1600$ mm. Therefore, this demonstrates that even a small height variation of 0.25 mm had a dramatic impact on the upstream displacement of the transition location compared to the first cases.

3.2 Spectra of velocity fluctuation

The velocity fluctuation signal was measured using hot-wire probe. The hot-wire probe was positioned within the boundary layer at a distance from the surface such that it measures approximately 40% of the free-stream velocity. To achieve this, the anemometer was calibrated in order to accurately determine this value, resulting in several in the y-position for each x-station due to the increasing boundary layer thickness along the length of the flat plate. This calibration was based on the Blasius profile experiment (Fig. 8). For post-processing of the signal, the Welch method, involving the averaging of spectra from subsets of the time signal, was employed to reduce spurious noise. The data acquisition was carried out in a free stream velocity of 27.1 m/s and was performed at 16 points along the plate. It began at $x = 640$, which is 10 mm from the trailing edge of the bump, and extended up to $x = 1900$ mm, close to the end of the plate. These points were spaced at 100 mm steps, starting at $x = 700$, except for the first three points, which are less spaced. The data acquisition lasted for 8 seconds with a sampling resolution of 8192 Hz. The variables shown in the following graphs are x (distance), f (frequency), and $\mathcal{F}(u'/U_\infty)$, which represents the Fourier transform and exhibits the signal amplitude. For the smooth case Fig. 11, the signal spectrum exhibits a dominant band between $100 \leq f$ Hz ≤ 400, which is defined as

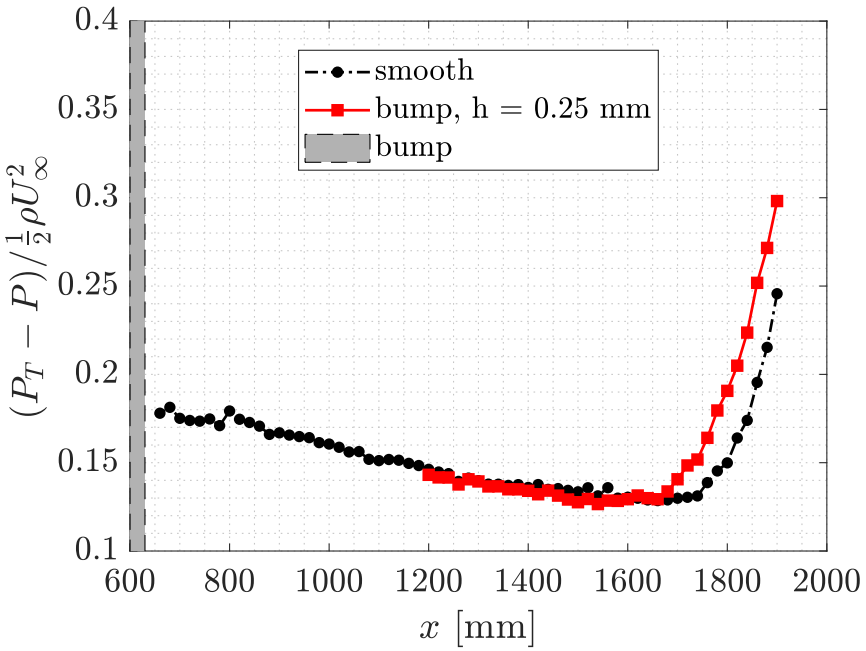

Figure 10. Measurement with Preston Tube for determine the transition location to a velocity of $U = 27.2m/s$.

the frequency band dominated by the TS wave. Therefore, this can be confirmed with linear instability theory, where it is identified that these frequencies are destabilizing and responsible for these perturbation waves. The amplification of the TS wave is progressive along x, revealing that in the transition regime of the boundary layer, all low and high-frequency bands start to amplify, causing the TS wave to be submerged among them. For the case with $h = 0.2$ mm, it can be noticed that this evolution was slightly more intense, with the spectra starting to become turbulent, indicating the onset of boundary layer transition.

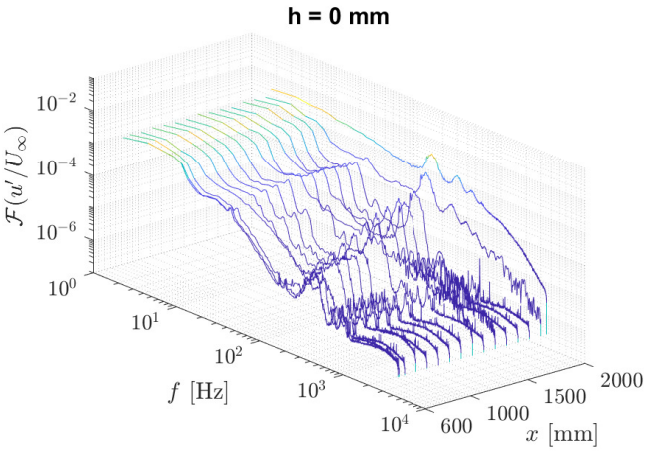

Figure 11. Growth of the TS wave along the x-axis for the smooth case.

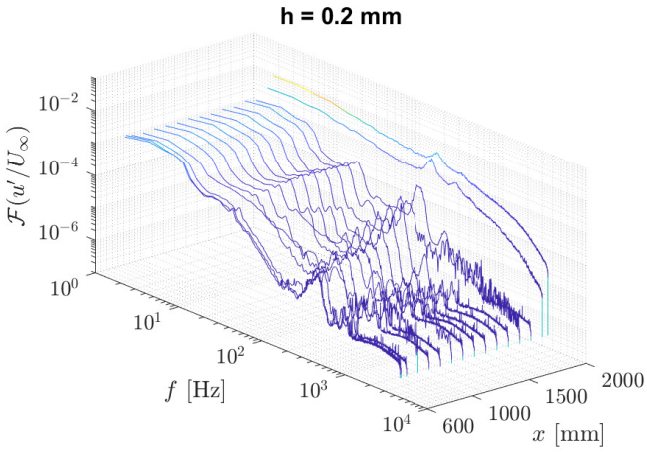

Figure 12. Growth of the TS wave along the x-axis for $h = 0.2$ mm.

It is evident from Fig.13 and Fig.14 that such evolution occurred more rapidly, which is why the transition location was displaced upstream. For the case $h = 0.4$, it can still be observed that the dominant band of the TS wave is growing up to station 14, and then in the last two stations, the boundary layer becomes entirely turbulent. In the other hand it is noticed that for a bump $h = 0.6$, the growth was more severe, with the TS wave growing only up to a few stations and then becoming fully turbulent from $x = 1500$ to trailing edge of the flat plate. This illustrates how a small bump accelerates the growth of the disturbance wave.

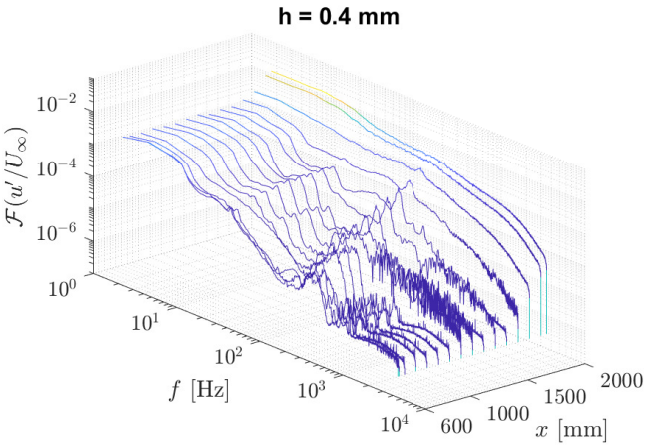

Figure 13. Growth of the TS wave along the x-axis for $h = 0.4$ mm.

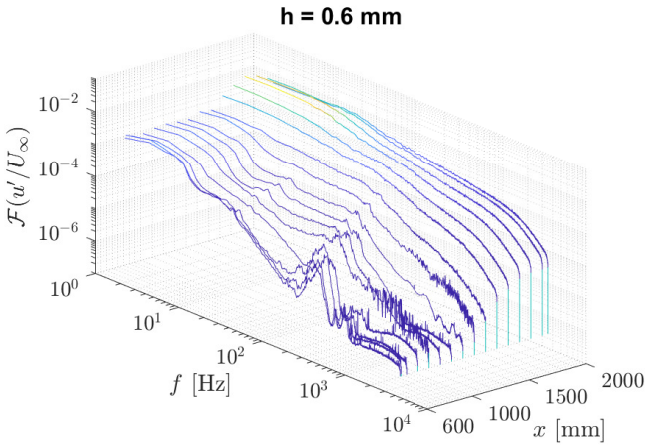

Figure 14. Growth of the TS wave along the x-axis for $h = 0.6$ mm.

4. CONCLUSIONS AND RECOMMENDATIONS

This paper presents experiments aimed at investigating the impact on boundary layer transition caused by bumps. The use of the Preston tube technique and hot-wire anemometry provided means to determine the transition location and the evolution of TS wave on the boundary layer, respectively. The results has showed significant variations in the estimated location of the transition point with different bump configurations, demonstrating a considerable effect as the height increases. Nonetheless, these findings could be more consistently corroborated through the application of linear instability theory, a topic not covered in this study.

For the initial Blasius profile experiment, it was evident that for different free stream velocities and various x-stations, the profiles followed the theoretical curve of the solution proposed by Blasius' equation. Since the experiments have been conducted on different days, the wind tunnel conditions have varied significantly, resulting in natural transition occurring at a speed of 27.2 m/s at $x = 1700$ mm, in an x-station that was not anticipated based on results from a different day using hot-wire anemometry. Therefore, a new verification can be conducted to evaluate result consistency.

In addition, it can also be observed that for bumps greater than 0.6 mm, there is an excessive growth of TS waves. Therefore, we could attribute this to the possibility of secondary instability modes or bypass transition. Even though these results are based on low-speed test conditions and small bumps, the basic methodology and bump characterization extends to higher-speed flows typical for commercial transport aircraft. There is a wide range of configurations that could be employed in the LANT wind tunnel to conduct bump experiments, which could involve increased height up to 20 mm and different velocities from 10 m/s to 30 m/s.

However, further research is needed to investigate the impact of TS wave evolution or whether other instability modes play a role in boundary layer transition. The spectral analysis revealed that the bump significantly affects the growth of TS waves, even altering the band of amplified frequencies. Ultimately, this topic is of great interest in the field of aeronautical engineering, particularly concerning drag reduction, as relatively small imperfections have a dramatic impact on boundary layer transition.

5. ACKNOWLEDGEMENTS

L.J.L.L. and V.B.V. thank the Coordenação de Aperfeiçoamento de Pessoal de Nível Superior (CAPES) for the doctoral and master's scholarships. M.A.F.M. acknowledges support from Conselho Nacional de Desenvolvimento Científico e Tecnológico (CNPq) under grant number 307956/2019-9, Agência de Financiamento de Estudos e Projetos (FINEP) under grant number 01-09-0334-04, Fundação de Amparo à Pesquisa do Estado de São Paulo (FAPESP) under grant number 2019/15336-7, The Boeing Company under grant number 2021-GT-353, and the US Air Force Office of Scientific Research (AFOSR) under grants FA9550-18-1-0112 and FA9550-23-1-0030, managed by Dr. Roger Greenwood.

6. REFERENCES

Amaral, F.R., 2021. "The low acoustic noise and turbulence wind tunnel of the university of sao paulo". *The Aeronautical Journal*, Vol. 126, pp. 1–33. doi:10.1017/aer.2021.80.

Crouch, J.D. and Kosorygin, V.S., 2020. "Surface step effects on boundary-layer transition dominated by tollmien–schlichting instability". *AIAA Journal*, Vol. 58, pp. 2943–2950. doi:10.2514/1.J058518. URL

https://doi.org/10.2514/1.J058518.

Dryden, H.L., 1949. "Review of published data on the effect of roughness on transition from laminar to turbulent flow". *National Advisory Committee for Aeronautics*, pp. 477–482.

Klebanoff, P.S. and Tidstrom, K.D., 1972. "Mechanism by which a twodimensional roughness element induces boundarylayer transition". *The Physics of Fluids*, Vol. 15, p. 1173–1178.

Morkovin, M.V., 1985. "Bypass transition to turbulence and research Desiderata". In *In NASA. Lewis Research Center Transition in Turbines*. pp. 161–204.

Reneaux, J., 2004. "Overview on drag reduction technologies for civil transport aircrafts". In *European Congress on Computational Methods in Applied Sciences and Engineering ECCOMAS 2004*.

Reshotko, E., 2001. "Transient growth: A factor in bypass transition". *Physics of Fluids*, Vol. 5, No. 13. doi: doi:10.1063/1.1358308.

Schlichting, H., 1933. "Laminare strahlausbreitung". *ZAMM - Zeitschrift Für Angewandte Mathematik Und Mechanik*, Vol. 13(4), p. 260–263. doi:10.1002/zamm.19330130403.

Schneider, W., 2001. "The importance of aerodynamics in the development of commercially successful transport aircraft". *Aerodynamic Drag Reduction Technologies*, pp. 9–16. doi:$10.1007/978 - 3 - 540 - 45359 - 8_2$.

Schubauer, G.B. and Skramstad, H.K., 1947. "Laminar boundary layer oscillations and transition on a flat plate". *Journal of research of the National Bureau of Standards*, Vol. 38, p. 251.

Smith, A.M.O. and Gamberony, N., 1956. "Transition, pressure gradient and estability theory". *Douglas Aircraft Company, El Segundo Division*.

Stuper, J., 1949. "The influence of surface irregularities on transition with various pressure gradients". *Division of Aeronautics, Australia*, Vol. 9.

Tani, I., Hama, R. and Mituisi, S., 1940. "On the permissible roughness in the laminar boundary layer,". *JAero. Res. Inst. Tokyo*.

Tollmien, W., 1928. "Über die entstehung der turbulenz. 1. mitteilung". *Nachrichten von der Gesellschaft der Wissenschaften zu Göttingen, Mathematisch-Physikalische Klasse*, Vol. 1929 (1928), pp. 21–44. URL http://eudml.org/doc/59276>.

van Ingen, J.L., 1956. "A suggested semi-empirical method for the calculation of the boundary layer transition region". *Delft University of Technology*.

Wang, Y.X. and Gaster, M., 2005. "Effect of surface steps on boundary layer transition". *Experiments in Fluids*, Vol. 39(4), p. 679–686. doi:10.1007/s00348-005-1011-7.

7. RESPONSIBILITY NOTICE

The authors are solely responsible for the printed material included in this paper.